*Chapter*

# ELECTRONIC PROPERTIES OF SINGLE AND DOUBLE WALL CARBON NANOTUBES

***Richard Pincak*[a]*, *Michal Pudlak*[a] *and Jan Smotlacha*[b]**
[a]Institute of Experimental Physics, Slovak Academy of Sciences,
Watsonova 47,043 53 Kosice, Slovak Republic
[b]Faculty of Nuclear Sciences and Physical Engineering,
Czech Technical University,
Brehova 7, 110 00 Prague, Czech Republic

**Abstract**

The electronic spectra of single wall and also double wall carbon nanotubes using tight binding approximation are investigated. We focus on the double wall zig-zag and armchair nanotubes. The influence of nanotube curvature on the electronic spectra is also treated. The impact of the external magnetic field on the spectral characteristic of double wall nanotubes is computed. The strong changes of the electronic spectra caused by the different geometry of the zig-zag and armchair nanotubes have strong impact on their character of conductivity. We found the big change of the electronic spectra for the double walled carbon nanotubes due to the external magnetic field. The difference in the Fermi energy between outer and inner nanotube for double wall carbon nanotubes was found which originate from the different hybridization of $\pi$ orbital. The spectral characteristics are very different for the double wall zig-zag and armchair

*E-mail address: pincak@saske.sk

nanotubes. The electronic states of finite length zig-zag single wall carbon nanotubes were treated. The analytical solutions for the electronic spectra in finite length zig-zag nanotubes were derived. It was shown that the static magnetic field in such systems can change the number of the edge states and also split the degeneracy of the edge states. The results of our calculations are presented analytically as well as numerically.

**PACS** 73.63.-b, 73.63.Fg, 73.22.-f.

**Keywords:** Nanotubes, electronic structure of nanoscale materials, edge states, magnetic field, conductivity, nanocrystals

# 1. Introduction

Carbon based materials has attracted scientific interest in recent years from both an experimental [1] and a theoretical viewpoint [2]. Among them carbon nanotubes are very interesting because of their unique mechanical and electronic properties. A single-wall carbon nanotube can be described as a graphene sheet rolled into a cylindrical shape so that the structure is one-dimensional with axial symmetry and in general exhibiting a spiral conformation called chirality. The electronic states of carbon nanotubes are classified by the chiral vector that assigns the diameter and chirality of the nanotubes. The primary symmetry classification of carbon nanotubes is either achiral or chiral. Achiral carbon nanotubes are defined by a carbon nanotube whose mirror images have an identical structure to the original one. There are only two cases of achiral nanotubes, armchair and zig-zag nanotubes. The names of armchair and zig-zag nanotubes arise from the shape of the cross-section ring at the edge of the nanotubes. Chiral nanotubes exhibit spiral symmetry whose mirror image cannot be superposed onto the original one. There is a variety of geometries in carbon nanotubes where the diameter, chirality and cap structures are different. The electronic structure of carbon nanotubes is derived by a simple tight-binding calculation for the $\pi$-electrons of carbon atoms. Of special interest is the prediction that the calculated electronic structure of a carbon nanotube can be either metallic or semiconducting, depending on its diameter and chirality. The energy gap for a semiconductor nanotube is inversely proportional to its diameter. The energy bands consist of a set of one-dimensional energy dispersion relations which are cross sections of those for two-dimensional graphite. To obtain explicit expressions for the dispersion relations, the simplest cases to consider are the nan-

otubes having the highest symmetry, e.g. highly symmetric achiral nanotubes. The miniaturization of the graphene-based electronic devices needs clarification of the effect of edges on the electronic structure of nanometer sized carbon based structures. There are two basic edge shapes which determine the properties of graphen ribbons. It was shown that ribbons with zig-zag edges posses localized edge states. In the ribbons with armchair edges such states do not exist [3]. The synthesis of double wall carbon nanotubes (DWCNT) has been reported recently [4, 5]. Their electronic structure was investigated by the local density approximation [6, 7, 8, 9, 10] and the tight-binding model [11, 12, 13, 14]. A similar method can be used to investigate the electronic spectra of the fullerene molecules [15, 16]. We are interested in the zigzag and armchair DWCNT's with a small radius. In these DWCNT's the difference of the Fermi levels of individual nanotubes has to be taken into account. We focus on $(9,0)-(18,0)$ zig-zag tubules and $(5,5)-(10,10)$ armchair tubules. They are the best matched double layer tubules. We are also interested about the length effect in the case of zig-zag single wall carbon nanotubes (SWCNT) which posses the edge states similar to zig-zag nanoribbons.

## 2. $(9,0)-(18,0)$ zigzag tubules in a static magnetic field

We investigate the zigzag nanotubes in a static magnetic field $\vec{B}$ parallel to the nanotube axis. We assume Hamiltonian for an electron in a potential $V(r)$ and in the magnetic field in the form

$$H = \frac{1}{2m}\left(\vec{p} - \frac{e}{c}\vec{A}\right)^2 + V \tag{1}$$

Potential $V(r)$ reflects the structure of the crystal lattice such as the symmetry and periodicity properties. Here this potential describes the structure of zig-zag DWCNT. Vector potential $\vec{A}$ in the Landau gauge can be expressed in the form [17]

$$\vec{A} = (\frac{\Phi}{L}, 0), \tag{2}$$

where $\Phi = B\pi r^2$ is the magnetic flux penetrating the cross section of carbon nanotube and $L = 2\pi r$ is a circumference of the nanotube ($r$-nanotube radius). Here coordinate $x$ is in the circumferential direction and coordinate $y$ denotes the direction parallel to nanotube axis. To describe the parameters which characterize the zig-zag tubules, we start from the graphene layer [18] where we

can define the vectors connecting the nearest neighbor carbon atoms for zig-zag nanotubes in the form:

$$\overrightarrow{\tau_1} = a(0; \frac{1}{\sqrt{3}}), \tag{3}$$

$$\overrightarrow{\tau_2} = a(\frac{1}{2}; -\frac{1}{2\sqrt{3}}), \tag{4}$$

$$\overrightarrow{\tau_3} = a(-\frac{1}{2}; -\frac{1}{2\sqrt{3}}). \tag{5}$$

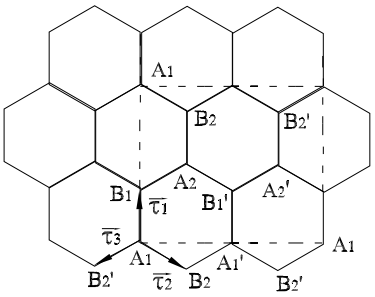


Figure 1. The outer shell part of the unit cell in the case of zigzag nanotubes.

The distance between atoms in the unit cell is $d = |\overrightarrow{\tau_i}| = \frac{a}{\sqrt{3}}$. Following the scheme in Figs. 1,2 [19] we want to find the solution to the double-layer graphene tubules in the form:

$$\psi(\overrightarrow{r}) = \psi^{out}(\overrightarrow{r}) + \psi^{in}(\overrightarrow{r}), \tag{6}$$

where

$$\begin{aligned}\psi^{out}(\overrightarrow{r}) = C_{A_1}\psi_{A_1} + C_{A_2}\psi_{A_2} + C_{B_1}\psi_{B_1} + C_{B_2}\psi_{B_2} \\ + C_{A_1^{'}}\psi_{A_1^{'}} + C_{A_2^{'}}\psi_{A_2^{'}} + C_{B_1^{'}}\psi_{B_1^{'}} + C_{B_2^{'}}\psi_{B_2^{'}},\end{aligned} \tag{7}$$

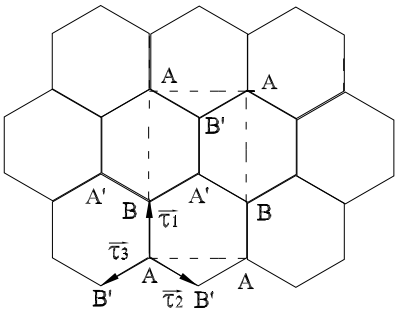


Figure 2. The inner shell part of the unit cell in the case of zig-zag nanotubes.

and

$$\psi^{in}(\overrightarrow{r}) = C_A\psi_A + C_B\psi_B + C_{A'}\psi_{A'} + C_{B'}\psi_{B'}. \tag{8}$$

We want to find the solution to the above problem in the form of the Bloch function

$$\psi_\alpha(\overrightarrow{k}, \overrightarrow{r}) = \tag{9}$$

$$= \frac{1}{\sqrt{M}} \sum_n \exp\left( i\overrightarrow{k}(\overrightarrow{r_n} + \overrightarrow{d}_\alpha) + i\frac{e}{c\hbar} G(\overrightarrow{r_n} + \overrightarrow{d}_\alpha) \right) |\varphi(\overrightarrow{r} - \overrightarrow{r}_n - \overrightarrow{d}_\alpha)\rangle,$$

where $\alpha$ denotes $A$ or $B$ atoms. Here $\overrightarrow{d}_\alpha$ are the coordinate of the $\alpha$ atom in the unit cell and $\overrightarrow{r_n}$ is a position of a unit cell, $M$ is the number of the unit cell; $|\varphi(\vec{r})\rangle$ is a $\pi$ orbital which is generally different for the outer and inner shell. $G(\vec{R})$ is the phase factor associated with the magnetic field and is expressed by [20]

$$G(\vec{R}) = \int_{\vec{R}}^{\vec{r}} \vec{A}(\vec{x}).d\vec{x} = \int_0^1 (\vec{r} - \vec{R}).\vec{A}(\vec{R} + \lambda(\vec{r} - \vec{R}))d\lambda \tag{10}$$

Employing Eq.(2), we get

$$G(\vec{R}) = \int_0^1 (\vec{r} - \vec{R}).(\frac{\Phi}{L}, 0)d\lambda = (x - X)\frac{\Phi}{L} \tag{11}$$

We denote

$$\epsilon = \langle \varphi^{out}(\vec{r} - \vec{A_i})|H|\varphi^{out}(\vec{r} - \vec{A_i})\rangle = \langle \varphi^{out}(\vec{r} - \vec{B_i})|H|\varphi^{out}(\vec{r} - \vec{B_i})\rangle, \quad (12)$$

$$\widetilde{\epsilon} = \langle \varphi^{in}(\vec{r} - \vec{A_i})|H|\varphi^{in}(\vec{r} - \vec{A_i})\rangle = \langle \varphi^{in}(\vec{r} - \vec{B_i})|H|\varphi^{in}(\vec{r} - \vec{B_i})\rangle. \quad (13)$$

Now we define the intratube hopping integrals

$$\langle \varphi^{out}(\vec{r} - \vec{A_1})|H|\varphi^{out}(\vec{r} - \vec{B_1})\rangle = \gamma_0, \quad (14)$$

$$\langle \varphi^{out}(\vec{r} - \vec{A_1})|H|\varphi^{out}(\vec{r} - \vec{B_2})\rangle = \langle \varphi^{out}(\vec{r} - \vec{A_1})|H|\varphi^{out}(\vec{r} - \vec{B_2'})\rangle = \gamma_0\beta, \quad (15)$$

and

$$\langle \varphi^{in}(\vec{r} - \vec{A})|H|\varphi^{in}(\vec{r} - \vec{B})\rangle = \gamma_0, \quad (16)$$

$$\langle \varphi^{in}(\vec{r} - \vec{A})|H|\varphi^{in}(\vec{r} - \vec{B'})\rangle = \gamma_0\widetilde{\beta}, \quad (17)$$

and the intertube hopping integrals

$$\langle \varphi^{out}(\vec{r} - \vec{R_i})|H|\varphi^{in}(\vec{r} - \vec{R_j})\rangle = W_{ij}, \quad (18)$$

where $\gamma_0$ is the hopping integral in the graphene and $\beta(\widetilde{\beta})$ is a part which depends on the surface curvature and will be computed later. $\epsilon$ and $\widetilde{\epsilon}$ are Fermi energies of the outer and inner nanotubes; $|\varphi^{out}(\vec{r} - \vec{R_i})\rangle$, $|\varphi^{in}(\vec{r} - \vec{R_j})\rangle$ are $\pi$ orbitals on site $i$ at the outer and on site $j$ at the inner tubes; $W_{ij}$ are the intertube hopping integrals which depend on the distance $d_{ij}$ and angle $\theta_{ij}$ between the $\pi_i$ and $\pi_j$ orbitals (see [21, 22, 23] for details).

$$W_{ij} = \frac{\gamma_0}{8}\cos(\theta_{ij})e^{(\xi - d_{ij})/\delta}, \quad (19)$$

where $\theta_{ij}$ is an angle between the *i*-th atom of the inner shell and the *j*-th atom of the outer shell, $d_{ij}$ is the interatom distance and $\xi$ is the intertube distance. The characteristic length $\delta = 0.45\mathring{A}$. So in the tight-binding approximation we get the systems of equations as shown in Appendix A. Firstly, we solve the equations in Appendix A assuming that $W_{ij}$ is the perturbation. So we can decouple these 12 equations. We get 8 equations for the outer shell and 4 for the inner shell. If we express the state of the outer shell (Eq.7) in the form $\psi^{out} = (C_{A_1}, C_{B_1}, C_{A_2}, C_{B_2}, C_{A_1'}, C_{B_1'}, C_{A_2'}, C_{B_2'})$, we get the solutions to the outer shell in the form

$$E_{1,2}(k) = \tag{20}$$

$$\epsilon \pm \gamma_0 \left(1 + 4\beta \cos\left(\frac{m\pi}{N} + \frac{\Phi}{N\Phi_0}\right) \cos\frac{\sqrt{3}ka}{2} + 4\beta^2 \cos^2\left(\frac{m\pi}{N} + \frac{\Phi}{N\Phi_0}\right)\right)^{\frac{1}{2}},$$

$$\psi_{1,2} = \frac{1}{\sqrt{8}}\left(1; \pm e^{-i\varphi_1}; 1; \pm e^{-i\varphi_1}, 1; \pm e^{-i\varphi_1}; 1; \pm e^{-i\varphi_1}\right) \tag{21}$$

$$E_{3,4}(k) = \tag{22}$$

$$\epsilon \pm \gamma_0 \left(1 - 4\beta \cos\left(\frac{m\pi}{N} + \frac{\Phi}{N\Phi_0}\right) \cos\frac{\sqrt{3}ka}{2} + 4\beta^2 \cos^2\left(\frac{m\pi}{N} + \frac{\Phi}{N\Phi_0}\right)\right)^{\frac{1}{2}},$$

$$\psi_{3,4} = \frac{1}{\sqrt{8}}\left(1; \pm e^{-i\varphi_2}; -1; \mp e^{-i\varphi_2}, 1; \pm e^{-i\varphi_2}; -1; \mp e^{-i\varphi_2}\right) \tag{23}$$

$$E_{5,6}(k) = \tag{24}$$

$$\epsilon \pm \gamma_0 \left(1 + 4\beta \sin\left(\frac{m\pi}{N} + \frac{\Phi}{N\Phi_0}\right) \cos\frac{\sqrt{3}ka}{2} + 4\beta^2 \sin^2\left(\frac{m\pi}{N} + \frac{\Phi}{N\Phi_0}\right)\right)^{\frac{1}{2}},$$

$$\psi_{5,6} = \frac{1}{\sqrt{8}}\left(1; \pm e^{-i\varphi_3}; -i; \mp ie^{-i\varphi_3}, -1; \mp e^{-i\varphi_3}; i; \pm ie^{-i\varphi_3}\right) \tag{25}$$

$$E_{7,8}(k) = \tag{26}$$

$$\epsilon \pm \gamma_0 \left(1 - 4\beta \sin\left(\frac{m\pi}{N} + \frac{\Phi}{N\Phi_0}\right) \cos\frac{\sqrt{3}ka}{2} + 4\beta^2 \sin^2\left(\frac{m\pi}{N} + \frac{\Phi}{N\Phi_0}\right)\right)^{\frac{1}{2}},$$

$$\psi_{7,8} = \frac{1}{\sqrt{8}}\left(1; \pm e^{-i\varphi_4}; i; \pm ie^{-i\varphi_4}, -1; \mp e^{-i\varphi_4}; -i; \mp ie^{-i\varphi_4}\right) \tag{27}$$

where, for instance,

$$e^{i\varphi_1} = \frac{e^{i\frac{ka}{\sqrt{3}}} + 2\beta \cos\left(\frac{m\pi}{N} + \frac{\Phi}{N\Phi_0}\right) e^{-i\frac{ka}{2\sqrt{3}}}}{\left(1 + 4\beta \cos\left(\frac{m\pi}{N} + \frac{\Phi}{N\Phi_0}\right) \cos\frac{\sqrt{3}ka}{2} + 4\beta^2 \cos^2\left(\frac{m\pi}{N} + \frac{\Phi}{N\Phi_0}\right)\right)^{\frac{1}{2}}}, \tag{28}$$

and $\Phi_0 = c\hbar/e$ is a flux quantum, $m = 0, 1, ..N-1$. Similar results for the electronic spectra in the case of inner nanotubes were found in the form $(\psi^{in} = (C_A, C_B, C_{A^`}, C_{B^`}))$

$$E_{9,10}(k) = \tag{29}$$

$$\tilde{\epsilon} \pm \gamma_0 \left(1 + 4\widetilde{\beta} \cos\left(\frac{m\pi}{N} + \frac{\Phi}{2N\Phi_0}\right) \cos\frac{\sqrt{3}ka}{2} + 4\widetilde{\beta}^2 \cos^2\left(\frac{m\pi}{N} + \frac{\Phi}{2N\Phi_0}\right)\right)^{\frac{1}{2}},$$

$$\psi_{9,10} = \frac{1}{\sqrt{4}}\left(1; \pm e^{-i\varphi_5}; 1; \pm e^{-i\varphi_5}\right) \tag{30}$$

$$E_{11,12}(k) = \tag{31}$$

$$\tilde{\epsilon} \pm \gamma_0 \left(1 - 4\widetilde{\beta} \cos\left(\frac{m\pi}{N} + \frac{\Phi}{2N\Phi_0}\right) \cos\frac{\sqrt{3}ka}{2} + 4\widetilde{\beta}^2 \cos^2\left(\frac{m\pi}{N} + \frac{\Phi}{2N\Phi_0}\right)\right)^{\frac{1}{2}},$$

$$\psi_{11,12} = \frac{1}{\sqrt{4}}\left(1; \pm e^{-i\varphi_6}; -1; \mp e^{-i\varphi_6}\right). \tag{32}$$

Since the radii of the outer and inner nanotubes are different, $\beta \neq \widetilde{\beta}$. Here $k_y = k$ and $-\frac{\pi}{\sqrt{3}a} < k < \frac{\pi}{\sqrt{3}a}$ is the first Brillouin zone. As we have a curved surface, the local normals on the neighboring sites are no longer perfectly aligned and this misorientation also changes the transfer integral. The change can be calculated using the curvature tensor $b_{\alpha\beta}$ [24]. The result is

$$\frac{\delta t_a}{t} = -\frac{1}{2} b_{\gamma\beta} b^{\gamma}_{\alpha} \tau^{\beta}_{a} \tau^{\alpha}_{a}, \tag{33}$$

where the only nonzero term is $b_{xx} b^{x}_{x} = 1/R^2$. So we have

$$\frac{\delta t_1}{t} = 0, \tag{34}$$

$$\frac{\delta t_2}{t} = -\frac{1}{2} b_{xx} b^{x}_{x} (\tau^{x}_{2})^2 = -\frac{1}{2R^2} (\tau^{x}_{2})^2, \tag{35}$$

$$\frac{\delta t_3}{t} = -\frac{1}{2} b_{xx} b^{x}_{x} (\tau^{x}_{3})^2 = -\frac{1}{2R^2} (\tau^{x}_{3})^2. \tag{36}$$

With using the unit vectors we have $(\tau^{x}_{2})^2$=$(\tau^{x}_{3})^2$=$\frac{a^2}{4}$. We found the radius of the inner nanotube from the expression $2\pi R = Na$. The nonzero terms are

$\frac{\delta t_2}{t} = \frac{\delta t_3}{t} = \frac{1}{2}(\frac{\pi}{N})^2$. The same holds for the outer nanotube. The parameters $\beta$, $\widetilde{\beta}$ can be expressed in the form

$$\widetilde{\beta} = 1 - \frac{\delta t_2}{t} = 1 - \frac{1}{2}(\frac{\pi}{9})^2 \tag{37}$$

and

$$\beta = 1 - \frac{\delta t_2}{t} = 1 - \frac{1}{2}(\frac{\pi}{18})^2. \tag{38}$$

Now we need the values $\epsilon$ and $\tilde{\epsilon}$ which are different because the inner and outer shell radii are different. Firstly we need to calculate the dependence of the $\pi$ orbital on the radius of the curvature. It was done in [25] to the lowest order in $a/R$

$$|\pi\rangle \approx \frac{a}{2\sqrt{6}R}|s\rangle + \frac{a}{4\sqrt{3}R}\,|p_y\rangle + |p_z\rangle, \tag{39}$$

and so we get

$$\varepsilon = \langle\pi|H|\pi\rangle \approx \frac{a^2}{24R^2}\langle s|H|s\rangle + \frac{a^2}{48R^2}\langle p_y|H|p_y\rangle + \langle p_z|H|p_z\rangle. \tag{40}$$

Due to $a/2R = \pi/N$,$(N = 9)$ we have

$$\tilde{\epsilon} = \frac{1}{6}\frac{\pi^2}{N^2}\langle s|H|s\rangle + \frac{1}{12}\frac{\pi^2}{N^2}\langle p_y|H|p_y\rangle + \langle p_z|H|p_z\rangle, \tag{41}$$

and

$$\epsilon = \frac{1}{24}\frac{\pi^2}{N^2}\langle s|H|s\rangle + \frac{1}{48}\frac{\pi^2}{N^2}\langle p_y|H|p_y\rangle + \langle p_z|H|p_z\rangle. \tag{42}$$

In the case $m = 3$ when we do not take into account the magnetic field $(B = 0)$ we find

$$E_{3,4}(k) = \epsilon \pm \gamma_0(1 - 2\beta\cos\frac{\sqrt{3}ka}{2} + \beta^2)^{\frac{1}{2}}, \tag{43}$$

$$E_{11,12}(k) = \tilde{\epsilon} \pm \gamma_0(1 - 2\widetilde{\beta}\cos\frac{\sqrt{3}ka}{2} + \widetilde{\beta}^2)^{\frac{1}{2}}, \tag{44}$$

where $k = 0$ is a Fermi point for both the inner and outer nanotubes in the case $\beta = \widetilde{\beta} = 1$. Nanotubes have no gap and have a semiconductor character. If we impose a curvature correction, we get a gap

$$E_g = 2\gamma_0(1 - \beta) = \gamma_0\left(\frac{\pi}{2N}\right)^2 = \frac{\gamma_0}{4}\left(\frac{a}{2R}\right)^2, \tag{45}$$

for the outer nanotube and

$$E_g = 2\gamma_0(1-\widetilde{\beta}) = \gamma_0\left(\frac{\pi}{N}\right)^2 = \frac{\gamma_0}{4}\left(\frac{a}{R}\right)^2, \tag{46}$$

for the inner nanotube. Here $R$ is the radius of the inner tube and $2R$ is the radius of the outer tube. So we get the same gap as was computed in [26] where the rehybridized orbital method was used. For $\gamma_0 \approx 3\ eV$ we get $E_g \approx 0.365\ eV$ for the inner tube and $E_g \approx 0.091\ eV$ for the outer tube. Now if the static magnetic field is imposed we get

$$E_g = 2\gamma_0|1-2\beta\cos\left(\pi/3+\Phi/N\Phi_0\right)| \tag{47}$$

for the outer nanotube and

$$E_g = 2\gamma_0|1-2\widetilde{\beta}\cos\left(\pi/3+\Phi/2N\Phi_0\right)| \tag{48}$$

for the inner nanotube. We can see that the magnetic field is changing the energy gap between valence and conductance band and the change is different for the inner and the outer tube.

Now we want to estimate the difference between "Fermi levels" of the inner and the outer shell. We have [27]

$$\langle s|H|s\rangle \approx -12eV, \tag{49}$$

$$\langle p_y|H|p_y\rangle \approx -4eV, \tag{50}$$

and the difference is

$$\epsilon-\tilde{\epsilon} = \frac{1}{6}\left(\left(\frac{\pi}{2N}\right)^2-\left(\frac{\pi}{N}\right)^2\right)\langle s|H|s\rangle+\frac{1}{12}\left(\left(\frac{\pi}{2N}\right)^2-\left(\frac{\pi}{N}\right)^2\right)\langle p_y|H|p_y\rangle. \tag{51}$$

From the expression above we finally get the value for the energy gap

$$\epsilon-\tilde{\epsilon} \approx 0.21eV. \tag{52}$$

Now we use the eigenstates $\psi_i$ to find the solution when the interaction between shells is imposed. We assume the symmetric geometry of zig-zag DWCNT. It means that the atoms $A$,$A_1$ and $B$,$B_1$ are directly one above another in the neighboring shells [13]. We take into account only the interactions

$$W_{A,A_1} = W_{B,B_1} = \frac{\gamma_0}{8}. \tag{53}$$

We look for solution in the form

$$\Psi = \sum_{i=1}^{12} \zeta_i \psi_i. \tag{54}$$

We have secular equations

$$\sum_{j=1}^{12} \langle \psi_i | H | \psi_j \rangle \zeta_j = \tilde{E} \zeta_i, \tag{55}$$

where

$$\langle \psi_i | H | \psi_j \rangle = \delta_{ij} E_i, \tag{56}$$

for diagonal matrix elements $i, j = 1, ...8$ and $i, j = 9, ...12$, and the interaction between shells (non diagonal matrix elements) is described by the terms $\langle \psi_i | H | \psi_j \rangle$ for $i = 1, ...8$ ; $j = 9, ...12$ and vice versa. We have, for instance,

$$\langle \psi_9 | H | \psi_1 \rangle = \frac{1}{4\sqrt{2}} \frac{\gamma_0}{8} \left( 1 + e^{i(\varphi_5 - \varphi_1)} \right), \tag{57}$$

$$\langle \psi_9 | H | \psi_2 \rangle = \frac{1}{4\sqrt{2}} \frac{\gamma_0}{8} \left( 1 - e^{i(\varphi_5 - \varphi_1)} \right). \tag{58}$$

We get the eigenvalues $\tilde{E}_i$ with eigenvectors which can be expressed in the form

$$\Psi_i = \sum_{j=1}^{12} \zeta_{i,j} \psi_j. \tag{59}$$

The eigenvalues of Eq.(56) for some values of $\sqrt{3}ka/2$ near the point $k = 0$ are depicted in Fig.(3) where $E_c$ and $E_v$ are conductive and valence band. When the static magnetic field is applying, the energy gap between valence and conductive band is significantly changing(see Figs.(4,5)). So the magnetic field influence the opto-electronic characteristics of this type of DWCNT's.

## 3. $(5,5) - (10,10)$ armchair tubules

We can make similar calculations of electronic spectra also in the case of armchair double-layer nanotubes. The system is characterized by the same type of Hamiltonian as in the previous section. Now the potential $V(r)$ reflects the

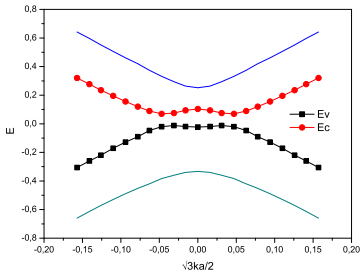


Figure 3. Spectra of zig-zag DWCNT with the intertube interactions.

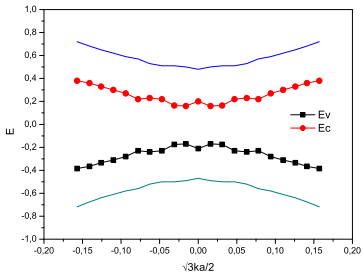


Figure 4. Spectra of zig-zag DWCNT with the intertube interactions when the static magnetic field $\Phi = 0.5\Phi_0$ is applied.

structure of armchair DWCNT. We can define the vectors connecting the nearest neighbor carbon atoms for armchair nanotubes in the form:

$$\overrightarrow{\tau_1} = a(\frac{1}{\sqrt{3}}; 0), \tag{60}$$

$$\overrightarrow{\tau_2} = a(-\frac{1}{2\sqrt{3}}; -\frac{1}{2}), \tag{61}$$

$$\overrightarrow{\tau_3} = a(-\frac{1}{2\sqrt{3}}; \frac{1}{2}). \tag{62}$$

The distance between atoms in the unit cell is also $|\overrightarrow{\tau_i}| = \frac{a}{\sqrt{3}}$. Now we define the intratube hopping integrals

$$\langle \varphi^{out}(r - A_1)|H|\varphi^{out}(r - B_1)\rangle = \gamma_0\alpha, \tag{63}$$

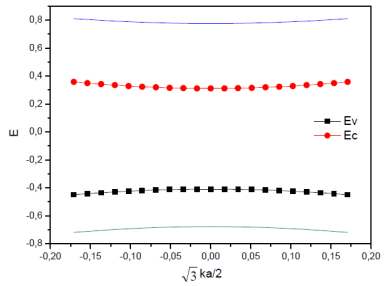


Figure 5. Spectra of zig-zag DWCNT with the intertube interactions when the static magnetic field $\Phi = 1\Phi_0$ is applied.

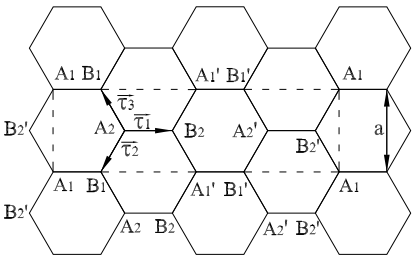


Figure 6. The outer shell part of the unit cell in the case of armchair nanotubes.

$$\langle \varphi^{out}(r - A_1)|H|\varphi^{out}(r - B_2^{'})\rangle = \gamma_0\beta, \tag{64}$$

and

$$\langle \varphi^{in}(r - A)|H|\varphi^{in}(r - B)\rangle = \gamma_0\widetilde{\alpha}, \tag{65}$$

$$\langle \varphi^{in}(r - A)|H|\varphi^{in}(r - B^{'})\rangle = \gamma_0\widetilde{\beta}, \tag{66}$$

where $\gamma_0$ is the hopping integral in the graphene and $\alpha(\widetilde{\alpha})$, $\beta(\widetilde{\beta})$ are parameters which describe the dependence of hopping integrals on the surface curvature. From Figures 6 and 7 we get the system of equations as described in Appendix B. At the beginning we neglect the intertube interactions in the equations described in Appendix B. We get a set of equations which can be decoupled. One set for the outer shell and the other for the inner shell. The electronic spectra

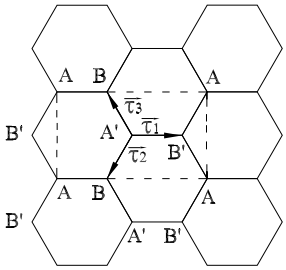


Figure 7. The inner shell part of the unit cell in the case of armchair nanotubes.

and eigenstate for the outer shell can be expressed in the form

$$E_{1,2}(k) = \epsilon \pm \gamma_0 \left( \alpha^2 + 4\alpha\beta \cos\left( \frac{m\pi}{5} + \frac{\Phi}{5\Phi_0} \right) \cos\frac{ka}{2} + 4\beta^2 \cos^2\frac{ka}{2} \right)^{\frac{1}{2}}, \tag{67}$$

$$\psi_{1,2} = \frac{1}{\sqrt{8}} \left( 1; \pm e^{-i\varphi_1}; 1; \pm e^{-i\varphi_1}, 1; \pm e^{-i\varphi_1}; 1; \pm e^{-i\varphi_1} \right) \tag{68}$$

$$E_{3,4}(k) = \epsilon \pm \gamma_0 \left( \alpha^2 - 4\alpha\beta \cos\left( \frac{m\pi}{5} + \frac{\Phi}{5\Phi_0} \right) \cos\frac{ka}{2} + 4\beta^2 \cos^2\frac{ka}{2} \right)^{\frac{1}{2}}, \tag{69}$$

$$\psi_{3,4} = \frac{1}{\sqrt{8}} \left( 1; \pm e^{-i\varphi_2}; -1; \mp e^{-i\varphi_2}, 1; \pm e^{-i\varphi_2}; -1; \mp e^{-i\varphi_2} \right) \tag{70}$$

$$E_{5,6}(k) = \epsilon \pm \gamma_0 \left( \alpha^2 + 4\alpha\beta \sin\left( \frac{m\pi}{5} + \frac{\Phi}{5\Phi_0} \right) \cos\frac{ka}{2} + 4\beta^2 \cos^2\frac{ka}{2} \right)^{\frac{1}{2}}, \tag{71}$$

$$\psi_{5,6} = \frac{1}{\sqrt{8}} \left( 1; \pm e^{-i\varphi_3}; -i; \mp ie^{-i\varphi_3}, -1; \mp e^{-i\varphi_3}; i; \pm ie^{-i\varphi_3} \right) \tag{72}$$

$$E_{7,8}(k) = \epsilon \pm \gamma_0 \left( \alpha^2 - 4\alpha\beta \sin\left( \frac{m\pi}{5} + \frac{\Phi}{5\Phi_0} \right) \cos\frac{ka}{2} + 4\beta^2 \cos^2\frac{ka}{2} \right)^{\frac{1}{2}}, \tag{73}$$

$$\psi_{7,8} = \frac{1}{\sqrt{8}} \left( 1; \pm e^{-i\varphi_4}; i; \pm ie^{-i\varphi_4}, -1; \mp e^{-i\varphi_4}; -i; \mp ie^{-i\varphi_4} \right). \tag{74}$$

The electronic spectra for the inner nanotubes was found in the form

$$E_{9,10}(k) = \tilde{\epsilon} \pm \gamma_0 \left( \widetilde{\alpha}^2 + 4\widetilde{\alpha}\widetilde{\beta} \cos\left( \frac{m\pi}{5} + \frac{\Phi}{10\Phi_0} \right) \cos\frac{ka}{2} + 4\widetilde{\beta}^2 \cos^2\frac{ka}{2} \right)^{\frac{1}{2}}, \tag{75}$$

$$\psi_{9,10} = \frac{1}{\sqrt{4}} \left( 1; \pm e^{-i\varphi_5}; 1; \pm e^{-i\varphi_5} \right) \tag{76}$$

$$E_{11,12}(k) = \tilde{\epsilon} \pm \gamma_0 \left( \widetilde{\alpha}^2 - 4\widetilde{\alpha}\widetilde{\beta} \cos\left( \frac{m\pi}{5} + \frac{\Phi}{10\Phi_0} \right) \cos\frac{ka}{2} + 4\widetilde{\beta}^2 \cos^2\frac{ka}{2} \right)^{\frac{1}{2}}, \tag{77}$$

$$\psi_{11,12} = \frac{1}{\sqrt{4}} \left( 1; \pm e^{-i\varphi_6}; -1; \mp e^{-i\varphi_6} \right). \tag{78}$$

From the boundary condition $k_x L = 2\pi m$, $L = N3d$ where $d = a/\sqrt{3}$ is the nearest neighbor bond length we get $k_x = \frac{2\pi m}{3dN} = \frac{2\pi m}{\sqrt{3}Na}$, $m = 0, 1, ...N-1$; $3d$ is the length of the unit cell in the x-direction. Here $k_y = k$ and $-\frac{\pi}{a} < k < \frac{\pi}{a}$ is the first Brillouin zone. In this case, we assume that $N = 5$ for the above spectrum. The value for the parameter $\widetilde{\alpha}$ and $\widetilde{\beta}$ can be found from the expressions $\widetilde{\alpha}$=1 $-\frac{1}{2} b_{xx} b_x^x (\tau_1^x)^2$=1-$\frac{1}{2R^2}\frac{a^2}{3}$ and $\widetilde{\beta}$=1 $-\frac{1}{2} b_{xx} b_x^x (\tau_2^x)^2$=1-$\frac{1}{2R^2}\frac{a^2}{12}$. The radius for the inner, outer nanotube can be found from the expressions $2\pi R = N3d = \sqrt{3}Na$, $2\pi R = N6d$, respectively. Now we make a correction of transfer integral caused by the curvature of nanotubes

$$\widetilde{\beta} = 1 - \frac{1}{2}(\frac{\pi}{3N})^2; \quad \beta = 1 - \frac{1}{8}(\frac{\pi}{3N})^2, \tag{79}$$

$$\widetilde{\alpha} = 1 - 2(\frac{\pi}{3N})^2; \quad \alpha = 1 - \frac{1}{2}(\frac{\pi}{3N})^2. \tag{80}$$

The $\pi$ orbital can be expressed in the form

$$|\pi\rangle \approx \frac{\sqrt{2}d}{4R}|s\rangle + \frac{d}{4R}|p_x\rangle + |p_z\rangle. \tag{81}$$

Due to $3dN = 2\pi R$ we get

$$|\pi\rangle \approx \frac{\sqrt{2}\pi}{6N}|s\rangle + \frac{\pi}{6N}|p_x\rangle + |p_z\rangle, \tag{82}$$

and so

$$\varepsilon = \langle\pi|H|\pi\rangle \approx \frac{1}{18}\left(\frac{\pi}{N}\right)^2 \langle s|H|s\rangle + \frac{1}{36}\left(\frac{\pi}{N}\right)^2 \langle p_x|H|p_x\rangle + \langle p_z|H|p_z\rangle. \tag{83}$$

From this expression we derive, if $N = 5$,

$$\tilde{\epsilon} = \frac{1}{18}\left(\frac{\pi}{N}\right)^2 \langle s|H|s\rangle + \frac{1}{36}\left(\frac{\pi}{N}\right)^2 \langle p_x|H|p_x\rangle + \langle p_z|H|p_z\rangle, \qquad (84)$$

and

$$\epsilon = \frac{1}{18}\left(\frac{\pi}{2N}\right)^2 \langle s|H|s\rangle + \frac{1}{36}\left(\frac{\pi}{2N}\right)^2 \langle p_x|H|p_x\rangle + \langle p_z|H|p_z\rangle. \qquad (85)$$

The energy levels $E_{3,4}$ and $E_{11,12}$ define the Fermi point for $m = 0$ in the case without magnetic field. We have

$$E_{3,4}(k) = \epsilon \pm \gamma_0 |\alpha - 2\beta \cos\frac{ka}{2}|, \qquad (86)$$

$$E_{11,12}(k) = \tilde{\epsilon} \pm \gamma_0 |\widetilde{\alpha} - 2\widetilde{\beta} \cos\frac{ka}{2}|, \qquad (87)$$

and the Fermi point is defined by the equations

$$\widetilde{\alpha} - 2\widetilde{\beta} \cos\frac{ka}{2} = 0, \qquad (88)$$

for the inner shell, and

$$\alpha - 2\beta \cos\frac{ka}{2} = 0, \qquad (89)$$

for the outer shell, respectively. By virtue of $\beta \geq \alpha(\tilde{\beta} \geq \tilde{\alpha})$ the curvature does not open a gap in the case of single nanotubes. When we impose the static magnetic field, the above equation get a form

$$E_{3,4}(k) = \epsilon \pm \gamma_0 |\alpha - 2\beta \cos(\Phi/5\Phi_0) \cos\frac{ka}{2}|, \qquad (90)$$

$$E_{11,12}(k) = \tilde{\epsilon} \pm \gamma_0 |\widetilde{\alpha} - 2\widetilde{\beta} \cos(\Phi/10\Phi_0) \cos\frac{ka}{2}| \qquad (91)$$

and the Fermi point is defined by the equations

$$\widetilde{\alpha} - 2\widetilde{\beta} \cos(\Phi/10\Phi_0) \cos\frac{ka}{2} = 0, \qquad (92)$$

for the inner shell and

$$\alpha - 2\beta \cos(\Phi/5\Phi_0) \cos\frac{ka}{2} = 0, \qquad (93)$$

for the outer shell. From Eq.(92) we get the following formula for the Fermi wave vector $k_F$ of the armchair SWCNT:

$$k_F = \frac{2}{a} \arccos \frac{1 - \frac{1}{2}\left(\frac{d}{R}\right)^2}{2\cos\left(\frac{3d\Phi}{4\pi R\Phi_0}\right)\left(1 - \frac{1}{8}\left(\frac{d}{R}\right)^2\right)}. \tag{94}$$

For a large radius the Fermi wave vector is located at $k_F(R \to \infty) = 2\pi/3a$. As a diameter decreases, the position of $k_F$ shifts from $k_F(R \to \infty)$ towards the bigger wave vectors. Strong enough magnetic field can open the gap between valence and conductive bands. Using the values $\langle s|H|s\rangle \approx -12eV$ and $\langle p_x|H|p_x\rangle \approx -4eV$ in the following expression:

$$\epsilon - \tilde{\epsilon} = \frac{1}{18}\left(\left(\frac{\pi}{2N}\right)^2 - \left(\frac{\pi}{N}\right)^2\right)\langle s|H|s\rangle + \frac{1}{36}\left(\left(\frac{\pi}{2N}\right)^2 - \left(\frac{\pi}{N}\right)^2\right)\langle p_x|H|p_x\rangle, \tag{95}$$

we find

$$\epsilon - \tilde{\epsilon} \approx 0.23\ eV. \tag{96}$$

Now we use the eigenstates $\psi_i$ to find the solution when the interaction between shells is imposed. Similarly, as in the previous case, we look for the solution in the form

$$\Psi = \sum_{i=1}^{12} \zeta_i \psi_i. \tag{97}$$

We have secular equations

$$\sum_{j=1}^{12} \langle \psi_i|H|\psi_j\rangle \zeta_j = \tilde{E}\zeta_i, \tag{98}$$

We take into account all intertube interactions between atoms which have a distance $d_{ij}$ less than $4.2\mathring{A}$ similarly as in [22, 23]. We use the value $\xi = 3.466$ for the intertube distance in the numerical computations. We compute spectra for symmetric geometry where the atoms $B_2^{'}(A_2)$ occupy a position directly above $A^{'}(B^{'})$,respectively. We get the eigenvalues $\tilde{E}_i$ with the eigenvectors which can be expressed in the form

$$\Psi_i = \sum_{j=1}^{12} \zeta_{i,j} \psi_j. \tag{99}$$

The spectra for some values of $ka/2$ near the Fermi points of single nanotubes are depicted in Figure 8. The point $ka/2 = 1.086$ is the Fermi point of the isolated inner nanotube. The point $ka/2 = 1.057$ is the Fermi point of the isolated outer nanotube. Approximately, from point $ka/2 = 1.054$ to point $1.095$ the $\tilde{E}_{11}$ levels are below the $\tilde{E}_4$ level. So in the armchair DWCNT the state $\Psi_{11}$ is occupied at these points. The state $\Psi_{11}$ is some mixture of the states $\psi_i$. For example, for the point $ka/2 = 1.083$ we have that the main part of $\Psi_{11}$ is $\psi_{11}$ which is $\pi^*$ state of the inner tube. We get that electrons which are localized in the outer nanotubes in the case without interaction between shells (or in the case of single nanotubes) are now localized in the inner nanotubes in the state which is unoccupied in the single nanotubes. When the static magnetic field is applied the character of conductivity is changing from semimetal to semiconductor (see Figs.9,10).

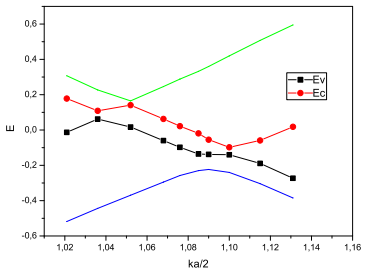


Figure 8. Spectra of armchair DWCNT with the intertube interactions without static magnetic field.

## 4. Edge States of Finite Length Zig-Zag Single Wall Carbon Nanotubes

Finite length open ended zig-zag carbon nanotubes can be assumed to be rolled from finite length zig-zag graphene nanoribbons [28]. In confining the structure along the length, the edge states are induced by terminating the length dimension with zig-zag shaped edges. The presence of edges in nanotube change the dimensionality of the system from one-dimensional to zero-dimensional system as is for instance the fullerene molecule [29]. We will study the edge and size

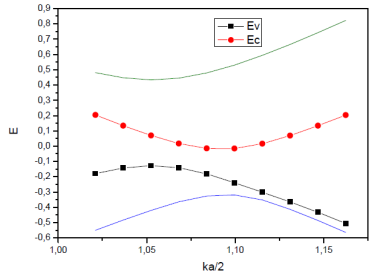


Figure 9. Spectra of armchair DWCNT with the intertube interactions when the static magnetic field $\Phi = 0.5\Phi_0$ is imposed.

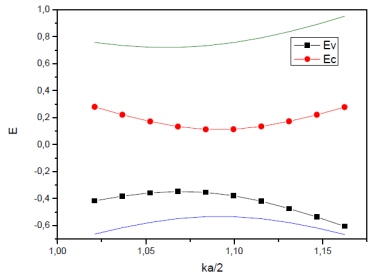


Figure 10. Spectra of armchair DWCNT with the intertube interactions when the static magnetic field $\Phi = 1\Phi_0$ is imposed.

effects using the tight-binding model for carbon nanotube shown in Fig. 11. The electronic spectrum of finite zig-zag single wall carbon nanotubes can be described by the following system of equations

$$\epsilon C_{A_m} + H_{A_m B_{m+1}} C_{B_{m+1}} + H_{A_m B_m} C_{B_m} = E C_{A_m}, \tag{100}$$

$$\epsilon C_{B_m} + H_{B_m A_{m-1}} C_{A_{m-1}} + H_{B_m A_m} C_{A_m} = E C_{B_m}, \tag{101}$$

where

$$H_{A_m B_{m+1}} = \gamma_0 \exp\left[i\left(k_x(\overrightarrow{\tau_1})_x + \frac{\Phi(\vec{\tau_1})_x}{L\Phi_0}\right)\right] = \gamma_0 \tag{102}$$

$$H_{A_m B_m} = \tag{103}$$

$$\gamma_0\beta\left(\exp\left[i\left(k_x(\overrightarrow{\tau_2})_x + \frac{\Phi(\vec{\tau_2})_x}{L\Phi_0}\right)\right] + \exp\left[i\left(k_x(\overrightarrow{\tau_3})_x + \frac{\Phi(\vec{\tau_3})_x}{L\Phi_0}\right)\right]\right) =$$

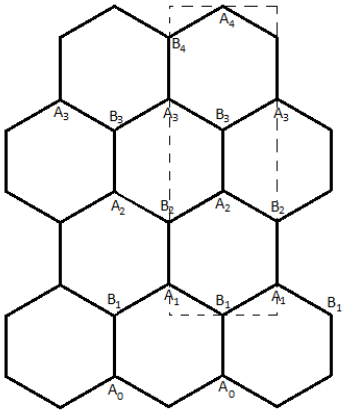


Figure 11. Structure of finite-length open ended single wall carbon nanotube with zig-zag edges. There is depicted a unit cell for width $M = 4$ which creates a nanotube.

$$= 2\gamma_0\beta\cos\left(\frac{n\pi}{N} + \frac{\Phi}{2N\Phi_0}\right),$$

where $n = 0, ....N-1$, $\beta = 1 - \frac{1}{2}\left(\frac{\pi}{N}\right)^2$ for $(N, 0)$ zig-zag nanotube(see Eq.(37))and site index $m = 1, ....., M+1$, where $M$ describes the length of the nanotube. So we have

$$\tilde{E}C_{A_m} + \gamma_0 C_{B_{m+1}} + g_n C_{B_m} = 0, \tag{104}$$

$$\tilde{E}C_{B_m} + \gamma_0 C_{A_{m-1}} + g_n C_{A_m} = 0, \tag{105}$$

where $\tilde{E} = \epsilon - E$ and $g_n = 2\gamma_0\beta\cos\left(\frac{n\pi}{N} + \frac{\Phi}{2N\Phi_0}\right)$. We assume that the $A_0$ and $B_{M+1}$ sites are missing. So we have the boundary condition $C_{A_0} = C_{B_{M+1}} = 0$ [3]. The solution is assumed to be (case I)

$$C_{A_m} = Ae^{ipm} + Be^{-ipm} \tag{106}$$

$$C_{B_m} = Ce^{ipm} + De^{-ipm} \tag{107}$$

Here $A, B, C$ and $D$ are coefficients which have to be determined and $p$ is the wavenumber in the direction of nanotube axis. From the boundary condition, we have

$$C_{A_0} = A + B = 0 \tag{108}$$

$$C_{B_{M+1}} = Ce^{ip(M+1)} + De^{-ip(M+1)} = 0 \tag{109}$$

And so

$$C_{A_m} = A(e^{ipm} - e^{-ipm}) \tag{110}$$

$$C_{B_m} = C(e^{ipm} - z^2 e^{-ipm}) \tag{111}$$

where $z = e^{ip(M+1)}$. Substituting the Eqs.(110,111) into Eqs.(104,105) we obtain

$$\tilde{E}\left(e^{ipm} - z^2 e^{-ipm}\right) C \tag{112}$$

$$+\left[\gamma_0\left(e^{ip(m-1)} - e^{-ip(m-1)}\right) + g_n\left(e^{ipm} - e^{-ipm}\right)\right] A = 0$$

$$\left[\gamma_0\left(e^{ip(m+1)} - z^2 e^{-ip(m+1)}\right) + g_n\left(e^{ipm} - z^2 e^{-ipm}\right)\right] C + \tag{113}$$

$$\tilde{E}\left(e^{ipm} - e^{-ipm}\right) A = 0$$

This homogenous system of equations has a solution only if the following condition is fulfilled

$$\left[\tilde{E}^2 - \left(\gamma_0 e^{-ip} + g_n\right)\left(\gamma_0 e^{ip} + g_n\right)\right] e^{2ipm} +$$

$$z^2\left[\tilde{E}^2 - \left(\gamma_0 e^{-ip} + g_n\right)\left(\gamma_0 e^{ip} + g_n\right)\right] e^{-2ipm} - \tag{114}$$

$$-\tilde{E}^2(z^2+1) + \left(g_n + \gamma_0 e^{ip}\right)^2 + z^2\left(g_n + \gamma_0 e^{-ip}\right)^2 = 0$$

And so the coefficient of $e^{\pm 2pm}$ terms and the constant term have to be equal to zero. Thus we obtain the energy spectrum

$$E = \epsilon + s\gamma_0\sqrt{1 + 4\beta\cos\left(\frac{n\pi}{N} + \frac{\Phi}{2N\Phi_0}\right)\cos(p) + 4\beta^2\cos^2\left(\frac{n\pi}{N} + \frac{\Phi}{2N\Phi_0}\right)} \tag{115}$$

Here, $s = \pm 1$, $s = +1$ ($s = -1$) corresponds to the conductance (valence) energy band. The condition for longitudinal wavenumber $p$ is

$$\tilde{E}^2(z^2+1) = \left(g_n + \gamma_0 e^{ip}\right)^2 + z^2\left(g_n + \gamma_0 e^{-ip}\right)^2 \tag{116}$$

Substituting Eq.(115) into Eq.(116) we obtain the equation which gives the longitudinal wavenumber $p$.

$$\sin[pM] + 2\beta\cos\left(\frac{n\pi}{N} + \frac{\Phi}{2N\Phi_0}\right)\sin[p(M+1)] = 0 \tag{117}$$

The longitudinal wavenumber depends on the transverse wavenumber $n$, on the length $M$ of the nanotube, on the static magnetic field $B$ and also on the parameter $\beta$ which depends on the nanotube curvature. For $N \gg 1$ Eq.(117) can be written as

$$\sin\left[pM\right] = 0 \tag{118}$$

The solution is given by

$$p = \frac{2\pi}{M} l \tag{119}$$

Substituting this solution into Eq.(115) we get the energy spectrum for infinite zig-zag nanotube with the periodic boundary condition along the y-axis. There is another possibility to solve Eqs.(104,105). We assume the solution in the form (case II)

$$C_{A_m} = (-1)^m \left(Ae^{ipm} + Be^{-ipm}\right) \tag{120}$$

$$C_{B_m} = (-1)^m \left(Ce^{ipm} + De^{-ipm}\right) \tag{121}$$

This possibility gives

$$E = \epsilon + s\gamma_0 \sqrt{1 - 4\beta\cos\left(\frac{n\pi}{N} + \frac{\Phi}{2N\Phi_0}\right)\cos(p) + 4\beta^2\cos^2\left(\frac{n\pi}{N} + \frac{\Phi}{2N\Phi_0}\right)} \tag{122}$$

and the equation for longitudinal wavenumber

$$\sin\left[pM\right] - 2\beta\cos\left(\frac{n\pi}{N} + \frac{\Phi}{2N\Phi_0}\right)\sin\left[p(M+1)\right] = 0 \tag{123}$$

Now we are interested about the edge state of zig-zag nanotube. This solution can be obtained in the form $p = \pi + i\eta$ [30]. We get the following equation for $\eta$:

$$\sinh\left[\eta M\right] \mp 2\beta\cos\left(\frac{n\pi}{N} + \frac{\Phi}{2N\Phi_0}\right)\sinh\left[\eta(M+1)\right] = 0 \tag{124}$$

The $-(+)$ sign is for the case I (II), respectively. The edge state can exist when the condition

$$|2\beta\cos\left(\frac{n\pi}{N} + \frac{\Phi}{2N\Phi_0}\right)| < \frac{1}{1+1/M} \tag{125}$$

is fulfilled. The energy spectrum of such state is given as

$$E_{n,s}(\Phi) = \tag{126}$$

$$\epsilon + s\gamma_0\sqrt{1 \mp 4\beta\cos\left(\frac{n\pi}{N} + \frac{\Phi}{2N\Phi_0}\right)\cosh(\eta) + 4\beta^2\cos^2\left(\frac{n\pi}{N} + \frac{\Phi}{2N\Phi_0}\right)}$$

For big enough $M$ the solution of Eq.(124) can be expressed in the form [30]

$$\eta = \ln\left[c_n + \frac{1 - c_n^2}{c_n^{2M+1}}\right] \tag{127}$$

where $1/c_n = |2\beta\cos\left(\frac{n\pi}{N} + \frac{\Phi}{2N\Phi_0}\right)|$. From Eq.(127) we have

$$\cosh\eta \approx \frac{1 + c_n^2}{2c_n} - \frac{\left(c_n^2 - 1\right)^2}{2c_n^{2M+3}} \tag{128}$$

and so

$$E_{n,s}(\Phi) \approx \epsilon + s\gamma_0\frac{c_n^2 - 1}{c_n^{M+2}} \tag{129}$$

for the solutions near the Fermi energy $\epsilon$. We can see that for long enough zig-zag nanotube the band gap becomes small. It means that we get energy level which is located in forbidden energy zone of the infinite zig-zag nanotube with periodic boundary conditions. So we have the HOMO (highest occupied molecular orbital)-LUMO (lowest unoccupied molecular orbital) gap for finite zig-zag nanotube in the form

$$E_g = 2\gamma_0\frac{c_{max}^2 - 1}{c_{max}^{M+2}} \tag{130}$$

where $c_{max}$ is maximal entity from $c_n$. The HOMO-LUMO gap is inversely proportional to the length of the zig-zag carbon nanotube. The similar result was found in the work [31]. Now for the sake of concreteness we focus on the finite $(9, 0)$ zig-zag nanotubes. In this case we get edge state for the value $n = 4$ in the case I and for the value $n = 6$ in the case II. Assuming $\epsilon = 0$ we have $E_{4,5,\pm}(0) = \pm 0.04meV$ for $M = 10$. The static magnetic field split the energy levels. We have $E_{4,\pm}(0.5\Phi_0) = \pm 0.15meV$ and $E_{5,\pm}(0.5\Phi_0) = \pm 0.007meV$. The presence of static magnetic field can change the number of edge states. Imposing the magnetic field $\Phi = 1\Phi_0$ we create a new edge state in the case I for $n = 3$ with energy $E_{3,\pm}(1\Phi_0) = \pm 161meV$ for $M = 10$ and $\pm 31meV$ for $M = 20$.

# 5. Conclusion

In the present work we investigate the influence of static magnetic field and also the presence of boundaries on the electronic properties of carbon nanotubes. We treat the single wall and also the double wall nanotubes. The Fermi levels of the individual nanotubes which create the double wall nanotubes are different. This difference is very important in the double wall nanotubes with small diameters. The interplay between energy difference of the Fermi levels of the individual nanotubes and the energy gap between valence and conducting band of individual nanotubes have a strong effect on the conductivity of double wall nanotubes [32, 33, 34]. We take into account the influence of a curvature of the surface on the matrix elements of the secular equation. The curvature of the surface opens the gap in the case of metallic zig-zag SWCNT's but does not open the gap in the case of metallic armchair SWCNT's. The Fermi level of the outer shell is about $0.21eV$ higher than the Fermi level of the inner shell in the case of $(9,0)-(18,0)$ zig-zag DWCNT's. In the case of zig-zag DWCNT's, the curvature does not shift the minimum of the conductance band and maximum of the valence band of the individual nanotubes. The result is that these DWCNT's are the semiconductor. The Fermi level of the outer shell is about $0.23eV$ higher than the Fermi level of the inner shell for $(5,5)-(10,10)$ armchair DWCNT's. The result is that in the armchair DWCNT's part of electrons from the valence band of the outer shell comes to the conductance band of the inner shell. The armchair DWCNT's have a semimetallic character. The static magnetic field changes the energy gap in the case of zig-zag carbon nanotubes but does not change the character of the conductivity. The zig-zag DWCNT remains the semiconductor also when the static magnetic field is applied. On the other hand in the case of the armchair nanotube the static magnetic field changes the character of the conductivity. The $(5,5)-(10,10)$ armchair DWCNT is semiconductor when enough strong static magnetic field is applied. The existence of the edge state in the case of finite length zig-zag nanotube results in the HOMO-LUMO gap which is inversely proportional to the length of the zig-zag nanotube. This gap can be smaller in comparison to the gap open by the curvature in the case of metallic single wall zig-zag nanotubes when the periodic boundary conditions are assumed. And so edge states change the electronic properties of zig-zag nanotubes. By imposing the static magnetic field we can change the number of the edge states. The magnetic field also split the energy degeneracy of the edge states.

# 6. Appendix A

In a tight-binding approximation for the case of zig-zag tubules we get the following systems of equations: for the outer shell

$$\epsilon C_{A_1}+H_{A_1B_2}C_{B_2}+H_{A_1B_2^{'}}C_{B_2^{'}}+H_{A_1B_1}C_{B_1}+\sum_{\lambda}W_{A_1,\lambda}C_{\lambda}=EC_{A_1}, \quad (131)$$

where $H_{A_1B_2}=\gamma_0\beta\exp\left[i\left(\overrightarrow{k}.\overrightarrow{\tau_2}+2\frac{\Phi(\vec{\tau_2})_x}{L\Phi_0}\right)\right]$; $H_{A_1B_2^{'}}=\gamma_0\beta\exp\left[i\left(\overrightarrow{k}.\overrightarrow{\tau_3}+2\frac{\Phi(\vec{\tau_3})_x}{L\Phi_0}\right)\right]$; $H_{A_1B_1}=\gamma_0\exp\left[i\left(\overrightarrow{k}.\overrightarrow{\tau_1}+2\frac{\Phi(\vec{\tau_1})_x}{L\Phi_0}\right)\right]$.

$$\epsilon C_{B_1}+H_{B_1A_1}C_{A_1}+H_{B_1A_2^{'}}C_{A_2^{'}}+H_{B_1A_2}C_{A_2}+\sum_{\lambda}W_{B_1,\lambda}C_{\lambda}=EC_{B_1}, \quad (132)$$

where $H_{B_1A_1}=\gamma_0\exp\left[-i\left(\overrightarrow{k}.\overrightarrow{\tau_1}+2\frac{\Phi(\vec{\tau_1})_x}{L\Phi_0}\right)\right]$; $H_{B_1A_2^{'}}=\gamma_0\beta\exp\left[-i\left(\overrightarrow{k}.\overrightarrow{\tau_2}+2\frac{\Phi(\vec{\tau_2})_x}{L\Phi_0}\right)\right]$; $H_{B_1A_2}=\gamma_0\beta\exp\left[-i\left(\overrightarrow{k}.\overrightarrow{\tau_3}+2\frac{\Phi(\vec{\tau_3})_x}{L\Phi_0}\right)\right]$.

$$\epsilon C_{A_2}+H_{A_2B_1}C_{B_1}+H_{A_2B_2}C_{B_2}+H_{A_2B_1^{'}}C_{B_1^{'}}+\sum_{\lambda}W_{A_2,\lambda}C_{\lambda}=EC_{A_2}, \quad (133)$$

where $H_{A_2B_2}=\gamma_0\exp\left[i\left(\overrightarrow{k}.\overrightarrow{\tau_1}+2\frac{\Phi(\vec{\tau_1})_x}{L\Phi_0}\right)\right]$; $H_{A_2B_1}=\gamma_0\beta\exp\left[i\left(\overrightarrow{k}.\overrightarrow{\tau_3}+2\frac{\Phi(\vec{\tau_3})_x}{L\Phi_0}\right)\right]$; $H_{A_2B_1^{'}}=\gamma_0\beta\exp\left[i\left(\overrightarrow{k}.\overrightarrow{\tau_2}+2\frac{\Phi(\vec{\tau_2})_x}{L\Phi_0}\right)\right]$.

$$\epsilon C_{B_2}+H_{B_2A_1}C_{A_1}+H_{B_2A_1^{'}}C_{A_1^{'}}+H_{B_2A_2}C_{A_2}+\sum_{\lambda}W_{B_2,\lambda}C_{\lambda}=EC_{B_2}, \quad (134)$$

where $H_{B_2A_1}=\gamma_0\beta\exp\left(-i\left(\overrightarrow{k}.\overrightarrow{\tau_2}+2\frac{\Phi(\vec{\tau_2})_x}{L\Phi_0}\right)\right)$; $H_{B_2A_1^{'}}=\gamma_0\beta\exp\left[-i\left(\overrightarrow{k}.\overrightarrow{\tau_3}+2\frac{\Phi(\vec{\tau_3})_x}{L\Phi_0}\right)\right]$; $H_{B_2A_2}=\gamma_0\exp\left[-i\left(\overrightarrow{k}.\overrightarrow{\tau_1}+2\frac{\Phi(\vec{\tau_1})_x}{L\Phi_0}\right)\right]$.

$$\epsilon C_{B_1^{'}}+H_{B_1^{'}A_2}C_{A_2}+H_{B_1^{'}A_2^{'}}C_{A_2^{'}}+H_{B_1^{'}A_1^{'}}C_{A_1^{'}}+\sum_{\lambda}W_{B_1^{'},\lambda}C_{\lambda}=EC_{B_1^{'}}, \quad (135)$$

where $H_{B_1^{'}A_2}=\gamma_0\beta\exp\left[-i\left(\overrightarrow{k}.\overrightarrow{\tau_2}+2\frac{\Phi(\vec{\tau_2})_x}{L\Phi_0}\right)\right]$; $H_{B_1^{'}A_2^{'}}=\gamma_0\beta\exp\left[-i\left(\overrightarrow{k}.\overrightarrow{\tau_3}+2\frac{\Phi(\vec{\tau_3})_x}{L\Phi_0}\right)\right]$; $H_{B_1^{'}A_1^{'}}=\gamma_0\exp\left[-i\left(\overrightarrow{k}.\overrightarrow{\tau_1}+2\frac{\Phi(\vec{\tau_1})_x}{L\Phi_0}\right)\right]$.

$$\epsilon C_{A_2^{'}}+H_{A_2^{'}B_1^{'}}C_{B_1^{'}}+H_{A_2^{'}B_2^{'}}C_{B_2^{'}}+H_{A_2^{'}B_1}C_{B_1}+\sum_{\lambda}W_{A_2^{'},\lambda}C_{\lambda}=EC_{A_2^{'}}, \quad (136)$$

where $H_{A_2^{'}B_1^{'}} = \gamma_0\beta\exp\left[i\left(\overrightarrow{k}.\overrightarrow{\tau_3}+2\frac{\Phi(\vec{\tau_3})_x}{L\Phi_0}\right)\right]$; $H_{A_2^{'}B_2^{'}} = \gamma_0\exp\left[i\left(\overrightarrow{k}.\overrightarrow{\tau_1}+2\frac{\Phi(\vec{\tau_1})_x}{L\Phi_0}\right)\right]$; $H_{A_2^{'}B_1} = \gamma_0\beta\exp\left[i\left(\overrightarrow{k}.\overrightarrow{\tau_2}+2\frac{\Phi(\vec{\tau_2})_x}{L\Phi_0}\right)\right]$.

$$\epsilon C_{B_2^{'}}+H_{B_2^{'}A_2^{'}}C_{A_2^{'}}+H_{B_2^{'}A_1^{'}}C_{A_1^{'}}+H_{B_2^{'}A_1}C_{A_1}+\sum_{\lambda}W_{B_2^{'},\lambda}C_{\lambda}=EC_{B_2^{'}}, \quad (137)$$

where $H_{B_2^{'}A_2^{'}} = \gamma_0\exp\left[-i\left(\overrightarrow{k}.\overrightarrow{\tau_1}+2\frac{\Phi(\vec{\tau_1})_x}{L\Phi_0}\right)\right]$; $H_{B_2^{'}A_1^{'}} = \gamma_0\beta\exp\left[-i\left(\overrightarrow{k}.\overrightarrow{\tau_2}+2\frac{\Phi(\vec{\tau_2})_x}{L\Phi_0}\right)\right]$; $H_{B_2^{'}A_1} = \gamma_0\beta\exp\left[-i\left(\overrightarrow{k}.\overrightarrow{\tau_3}+2\frac{\Phi(\vec{\tau_3})_x}{L\Phi_0}\right)\right]$.

$$\epsilon C_{A_1^{'}}+H_{A_1^{'}B_1^{'}}C_{B_1^{'}}+H_{A_1^{'}B_2}C_{B_2}+H_{A_1^{'}B_2^{'}}C_{B_2^{'}}+\sum_{\lambda}W_{A_1^{'},\lambda}C_{\lambda}=EC_{A_1^{'}}, \quad (138)$$

where $H_{A_1^{'}B_1^{'}} = \gamma_0\exp\left[i\left(\overrightarrow{k}.\overrightarrow{\tau_1}+2\frac{\Phi(\vec{\tau_1})_x}{L\Phi_0}\right)\right]$; $H_{A_1^{'}B_2} = \gamma_0\beta\exp\left[i\left(\overrightarrow{k}.\overrightarrow{\tau_3}+2\frac{\Phi(\vec{\tau_3})_x}{L\Phi_0}\right)\right]$; $H_{A_1^{'}B_2^{'}} = \gamma_0\beta\exp\left[i\left(\overrightarrow{k}.\overrightarrow{\tau_2}+2\frac{\Phi(\vec{\tau_2})_x}{L\Phi_0}\right)\right]$. Here $\lambda$ denotes the atoms of the unitary cell localized on the inner shell. Now we write down the equations for the inner shell in the case of zigzag nanotubes.

$$\tilde{\epsilon}C_A+H_{AB}C_B+H_{AB^{'}}C_{B^{'}}+\sum_{\lambda}W_{A,\lambda}C_{\lambda}=EC_A, \quad (139)$$

where $H_{AB}=\gamma_0\exp\left[i\left(\overrightarrow{k}.\overrightarrow{\tau_1}+\frac{\Phi(\vec{\tau_1})_x}{L\Phi_0}\right)\right]$;
$H_{AB^{'}}=\gamma_0\widetilde{\beta}\left(\exp\left[i\left(\overrightarrow{k}.\overrightarrow{\tau_2}+\frac{\Phi(\vec{\tau_2})_x}{L\Phi_0}\right)\right]+\exp\left[i\left(\overrightarrow{k}.\overrightarrow{\tau_3}+\frac{\Phi(\vec{\tau_3})_x}{L\Phi_0}\right)\right]\right)$.

$$\tilde{\epsilon}C_B+H_{BA}C_A+H_{BA^{'}}C_{A^{'}}+\sum_{\lambda}W_{B,\lambda}C_{\lambda}=EC_B, \quad (140)$$

where $H_{BA}=\gamma_0\exp\left[-i\left(\overrightarrow{k}.\overrightarrow{\tau_1}+\frac{\Phi(\vec{\tau_1})_x}{L\Phi_0}\right)\right]$;
$H_{BA^{'}}=\gamma_0\widetilde{\beta}\left(\exp\left[-i\left(\overrightarrow{k}.\overrightarrow{\tau_2}+\frac{\Phi(\vec{\tau_2})_x}{L\Phi_0}\right)\right]+\exp\left[-i\left(\overrightarrow{k}.\overrightarrow{\tau_3}+\frac{\Phi(\vec{\tau_3})_x}{L\Phi_0}\right)\right]\right)$.

$$\tilde{\epsilon}C_{A^{'}}+H_{A^{'}B}C_B+H_{A^{'}B^{'}}C_{B^{'}}+\sum_{\lambda}W_{A^{'},\lambda}C_{\lambda}=EC_{A^{'}}, \quad (141)$$

where $H_{A^{`}B^{`}} = \gamma_0 \exp\left[i\left(\overrightarrow{k}.\overrightarrow{\tau_1} + \frac{\Phi(\vec{\tau_1})_x}{L\Phi_0}\right)\right]$;
$H_{A^{`}B} = \gamma_0\widetilde{\beta}\left(\exp\left[i\left(\overrightarrow{k}.\overrightarrow{\tau_2} + \frac{\Phi(\vec{\tau_2})_x}{L\Phi_0}\right)\right] + \exp\left[i\left(\overrightarrow{k}.\overrightarrow{\tau_3} + \frac{\Phi(\vec{\tau_3})_x}{L\Phi_0}\right)\right]\right)$.

$$\tilde{\epsilon}C_{B^{`}} + H_{B^{`}A}C_A + H_{B^{`}A^{`}}C_{A^{`}} + \sum_{\lambda} W_{B^{`},\lambda}C_\lambda = EC_{B^{`}}, \qquad (142)$$

where $H_{B^{`}A^{`}} = \gamma_0 \exp\left[-i\left(\overrightarrow{k}.\overrightarrow{\tau_1} + \frac{\Phi(\vec{\tau_1})_x}{L\Phi_0}\right)\right]$;
$H_{B^{`}A} = \gamma_0\widetilde{\beta}\left(\exp\left[-i\left(\overrightarrow{k}.\overrightarrow{\tau_2} + \frac{\Phi(\vec{\tau_2})_x}{L\Phi_0}\right)\right] + \exp\left[-i\left(\overrightarrow{k}.\overrightarrow{\tau_3} + \frac{\Phi(\vec{\tau_3})_x}{L\Phi_0}\right)\right]\right)$ and $\lambda$ denotes the atoms of the unitary cell localized on the outer shell.

# 7. Appendix B

In a tight-binding approximation for the case of armchair tubules we get the following systems of equations: for the outer shell

$$\epsilon C_{A_1} + H_{A_1B_1}C_{B_1} + H_{A_1B_2^{`}}C_{B_2^{`}} + \sum_{\lambda} W_{A_1,\lambda}C_\lambda = EC_{A_1}, \qquad (143)$$

where $H_{A_1B_1} = \gamma_0\alpha \exp\left[i\left(\overrightarrow{k}.\overrightarrow{\tau_1} + 2\frac{\Phi(\vec{\tau_1})_x}{L\Phi_0}\right)\right]$;
$H_{A_1B_2^{`}} = \gamma_0\beta\left(\exp\left[i\left(\overrightarrow{k}.\overrightarrow{\tau_2} + 2\frac{\Phi(\vec{\tau_2})_x}{L\Phi_0}\right)\right] + \exp\left[i\left(\overrightarrow{k}.\overrightarrow{\tau_3} + 2\frac{\Phi(\vec{\tau_3})_x}{L\Phi_0}\right)\right]\right)$.

$$\epsilon C_{B_1} + H_{B_1A_1}C_{A_1} + H_{B_1A_2}C_{A_2} + \sum_{\lambda} W_{B_1,\lambda}C_\lambda = EC_{B_1}, \qquad (144)$$

where $H_{B_1A_1} = \gamma_0\alpha \exp\left[-i\left(\overrightarrow{k}.\overrightarrow{\tau_1} + 2\frac{\Phi(\vec{\tau_1})_x}{L\Phi_0}\right)\right]$;
$H_{B_1A_2} = \gamma_0\beta\left(\exp\left[-i\left(\overrightarrow{k}.\overrightarrow{\tau_2} + 2\frac{\Phi(\vec{\tau_2})_x}{L\Phi_0}\right)\right] + \exp\left[-i\left(\overrightarrow{k}.\overrightarrow{\tau_3} + 2\frac{\Phi(\vec{\tau_3})_x}{L\Phi_0}\right)\right]\right)$.

$$\epsilon C_{A_2} + H_{A_2B_2}C_{B_2} + H_{A_2B_1}C_{B_1} + \sum_{\lambda} W_{A_2,\lambda}C_\lambda = EC_{A_2}, \qquad (145)$$

where $H_{A_2B_2} = \gamma_0\alpha \exp\left[i\left(\overrightarrow{k}.\overrightarrow{\tau_1} + 2\frac{\Phi(\vec{\tau_1})_x}{L\Phi_0}\right)\right]$;
$H_{A_2B_1} = \gamma_0\beta\left(\exp\left[i\left(\overrightarrow{k}.\overrightarrow{\tau_2} + 2\frac{\Phi(\vec{\tau_2})_x}{L\Phi_0}\right)\right] + \exp\left[i\left(\overrightarrow{k}.\overrightarrow{\tau_3} + 2\frac{\Phi(\vec{\tau_3})_x}{L\Phi_0}\right)\right]\right)$.

$$\epsilon C_{B_2} + H_{B_2A_1^{`}}C_{A_1^{`}} + H_{B_2A_2}C_{A_2} + \sum_{\lambda} W_{B_2,\lambda}C_\lambda = EC_{B_2}, \qquad (146)$$

where $H_{B_2A_2} = \gamma_0\alpha \exp\left[-i\left(\overrightarrow{k}.\overrightarrow{\tau_1} + 2\frac{\Phi(\vec{\tau_1})_x}{L\Phi_0}\right)\right]$;
$H_{B_2A_1^{'}} = \gamma_0\beta\left(\exp\left[-i\left(\overrightarrow{k}.\overrightarrow{\tau_2} + 2\frac{\Phi(\vec{\tau_2})_x}{L\Phi_0}\right)\right] + \exp\left[-i\left(\overrightarrow{k}.\overrightarrow{\tau_3} + 2\frac{\Phi(\vec{\tau_3})_x}{L\Phi_0}\right)\right]\right)$.

$$\epsilon C_{A_1^{'}} + H_{A_1^{'}B_2}C_{B_2} + H_{A_1^{'}B_1^{'}}C_{B_1^{'}} + \sum_{\lambda} W_{A_1^{'},\lambda}C_{\lambda} = EC_{A_1^{'}}, \tag{147}$$

where $H_{A_1^{'}B_1^{'}} = \gamma_0\alpha \exp\left[i\left(\overrightarrow{k}.\overrightarrow{\tau_1} + 2\frac{\Phi(\vec{\tau_1})_x}{L\Phi_0}\right)\right]$;
$H_{A_1^{'}B_2} = \gamma_0\beta\left(\exp\left[i\left(\overrightarrow{k}.\overrightarrow{\tau_2} + 2\frac{\Phi(\vec{\tau_2})_x}{L\Phi_0}\right)\right] + \exp\left[i\left(\overrightarrow{k}.\overrightarrow{\tau_3} + 2\frac{\Phi(\vec{\tau_3})_x}{L\Phi_0}\right)\right]\right)$.

$$\epsilon C_{B_1^{'}} + H_{B_1^{'}A_1^{'}}C_{A_1^{'}} + H_{B_1^{'}A_2^{'}}C_{A_2^{'}} + \sum_{\lambda} W_{B_1^{'},\lambda}C_{\lambda} = EC_{B_1^{'}}, \tag{148}$$

where $H_{B_1^{'}A_1^{'}} = \gamma_0\alpha \exp\left[-i\left(\overrightarrow{k}.\overrightarrow{\tau_1} + 2\frac{\Phi(\vec{\tau_1})_x}{L\Phi_0}\right)\right]$;
$H_{B_1^{'}A_2^{'}} = \gamma_0\beta\left(\exp\left[-i\left(\overrightarrow{k}.\overrightarrow{\tau_2} + 2\frac{\Phi(\vec{\tau_2})_x}{L\Phi_0}\right)\right] + \exp\left[-i\left(\overrightarrow{k}.\overrightarrow{\tau_3} + 2\frac{\Phi(\vec{\tau_3})_x}{L\Phi_0}\right)\right]\right)$.

$$\epsilon C_{A_2^{'}} + H_{A_2^{'}B_1^{'}}C_{B_1^{'}} + H_{A_2^{'}B_2^{'}}C_{B_2^{'}} + \sum_{\lambda} W_{B_2^{'},\lambda}C_{\lambda} = EC_{B_2^{'}}, \tag{149}$$

where $H_{A_2^{'}B_2^{'}} = \gamma_0\alpha \exp\left[i\left(\overrightarrow{k}.\overrightarrow{\tau_1} + 2\frac{\Phi(\vec{\tau_1})_x}{L\Phi_0}\right)\right]$;
$H_{A_2^{'}B_1^{'}} = \gamma_0\beta\left(\exp\left[i\left(\overrightarrow{k}.\overrightarrow{\tau_2} + 2\frac{\Phi(\vec{\tau_2})_x}{L\Phi_0}\right)\right] + \exp\left[i\left(\overrightarrow{k}.\overrightarrow{\tau_3} + 2\frac{\Phi(\vec{\tau_3})_x}{L\Phi_0}\right)\right]\right)$.

$$\epsilon C_{B_2^{'}} + H_{B_2^{'}A_1}C_{A_1} + H_{B_2^{'}A_2^{'}}C_{A_2^{'}} + \sum_{\lambda} W_{B_2^{'},\lambda}C_{\lambda} = EC_{B_2^{'}}, \tag{150}$$

where $H_{B_2^{'}A_2^{'}} = \gamma_0\alpha \exp\left[-i\left(\overrightarrow{k}.\overrightarrow{\tau_1} + 2\frac{\Phi(\vec{\tau_1})_x}{L\Phi_0}\right)\right]$;
$H_{B_2^{'}A_1} = \gamma_0\beta\left(\exp\left[-i\left(\overrightarrow{k}.\overrightarrow{\tau_2} + 2\frac{\Phi(\vec{\tau_2})_x}{L\Phi_0}\right)\right] + \exp\left[-i\left(\overrightarrow{k}.\overrightarrow{\tau_3} + 2\frac{\Phi(\vec{\tau_3})_x}{L\Phi_0}\right)\right]\right)$.
Here $\lambda$ denotes the atoms of the unitary cell localized on the inner shell. The equations for the inner shell can be expressed in the form:

$$\tilde{\epsilon}C_A + H_{AB^{'}}C_{B^{'}} + H_{AB}C_B + \sum_{\lambda} W_{A,\lambda}C_{\lambda} = EC_A, \tag{151}$$

where $H_{AB} = \gamma_0\widetilde{\alpha} \exp\left[i\left(\overrightarrow{k}.\overrightarrow{\tau_1} + \frac{\Phi(\vec{\tau_1})_x}{L\Phi_0}\right)\right]$;
$H_{AB^{'}} = \gamma_0\widetilde{\beta}\left(\exp\left[i\left(\overrightarrow{k}.\overrightarrow{\tau_2} + \frac{\Phi(\vec{\tau_2})_x}{L\Phi_0}\right)\right] + \exp\left[i\left(\overrightarrow{k}.\overrightarrow{\tau_3} + \frac{\Phi(\vec{\tau_3})_x}{L\Phi_0}\right)\right]\right)$.

$$\tilde{\epsilon}C_B + H_{BA}C_A + H_{BA^{'}}C_{A^{'}} + \sum_{\lambda} W_{B,\lambda}C_{\lambda} = EC_B, \tag{152}$$

where $H_{BA} = \gamma_0 \widetilde{\alpha} \exp\left[-i\left(\overrightarrow{k}.\overrightarrow{\tau_1} + \frac{\Phi(\vec{\tau_1})_x}{L\Phi_0}\right)\right]$;
$H_{BA^{`}} = \gamma_0 \widetilde{\beta}\left(\exp\left[-i\left(\overrightarrow{k}.\overrightarrow{\tau_2} + \frac{\Phi(\vec{\tau_2})_x}{L\Phi_0}\right)\right] + \exp\left[-i\left(\overrightarrow{k}.\overrightarrow{\tau_3} + \frac{\Phi(\vec{\tau_3})_x}{L\Phi_0}\right)\right]\right)$.

$$\tilde{\epsilon} C_{A^{`}} + H_{A^{`}B} C_B + H_{A^{`}B^{`}} C_{B^{`}} + \sum_{\lambda} W_{A^{`},\lambda} C_{\lambda} = E C_{A^{`}}, \qquad (153)$$

where $H_{A^{`}B^{`}} = \gamma_0 \widetilde{\alpha} \exp\left[i\left(\overrightarrow{k}.\overrightarrow{\tau_1} + \frac{\Phi(\vec{\tau_1})_x}{L\Phi_0}\right)\right]$;
$H_{A^{`}B} = \gamma_0 \widetilde{\beta}\left(\exp\left[i\left(\overrightarrow{k}.\overrightarrow{\tau_2} + \frac{\Phi(\vec{\tau_2})_x}{L\Phi_0}\right)\right] + \exp\left[i\left(\overrightarrow{k}.\overrightarrow{\tau_3} + \frac{\Phi(\vec{\tau_3})_x}{L\Phi_0}\right)\right]\right)$.

$$\tilde{\epsilon} C_{B^{`}} + H_{B^{`}A} C_A + H_{B^{`}A^{`}} C_{A^{`}} + \sum_{\lambda} W_{B^{`},\lambda} C_{\lambda} = E C_{B^{`}}, \qquad (154)$$

where $H_{B^{`}A^{`}} = \gamma_0 \widetilde{\alpha} \exp\left[-i\left(\overrightarrow{k}.\overrightarrow{\tau_1} + \frac{\Phi(\vec{\tau_1})_x}{L\Phi_0}\right)\right]$;
$H_{B^{`}A} = \gamma_0 \widetilde{\beta}\left(\exp\left[-i\left(\overrightarrow{k}.\overrightarrow{\tau_2} + \frac{\Phi(\vec{\tau_2})_x}{L\Phi_0}\right)\right] + \exp\left[-i\left(\overrightarrow{k}.\overrightarrow{\tau_3} + \frac{\Phi(\vec{\tau_3})_x}{L\Phi_0}\right)\right]\right)$.
Here $\lambda$ denotes the atoms of the unitary cell localized on the outer shell.

**Acknowledgment**

The work was supported by the Slovak Academy of Sciences in the framework of CEX NANOFLUID, and by the Science and Technology Assistance Agency under Contract No. APVV 0509-07 , 0171 10, VEGA Grant No. 2/0069/10 and Ministry of Education Agency for Structural Funds of EU in frame of project 26220120021.

# References

[1] A.H.Castro Neto, F.Guinea, N.M.R.Peres, K.S.Novoselov and A.K.Geim, *Rev.Mod.Physics* 81 (**2009**) 109

[2] T.Ando, *J.Phys.Soc.Japan* 74 (**2005**) 777

[3] K.Wakabayashi, K.Sasaki, T.Nakanishi and T.Enoki, *Sci. Technol. Adv. Mater* 11 (**2010**) 054504

[4] T.Sugai, H.Yoshida, T.Shimada, T.Okazaki, H.Shinohara, *Nano Lett.* 3 (**2003**) 769

[5] Z.Zhou *et al.*, *Carbon* 41 (**2003**) 337

[6] Y.Kwon,D.Tomanek, *Phys.Rev. B* 58 (**1998**) R16001

[7] Y.Miyamoto,S.Saito,D.Tomanek, *Phys.Rev. B* 65 (**2001**) 041402(R)

[8] S.Okada,A.Oshiyama, *Phys.Rev. Lett*. 91 (**2003**) 216801

[9] V.Zólyomi,J.Koltai,Á.Rusznyák,J.Kürti,Á.Gali,F.Simon,H.Kuzmany,Á.Szabados and P.R.Surján, *Phys.Rev.B* 77 (**2008**) 245403

[10] V.Zólyomi,Á.Rusznyák,J.Kürti,Á.Gali,F.Simon,H.Kuzmany,Á.Szabados and P.R.Surján,*phys.stat.sol. (b)* 243 (**2006**) 3476

[11] Y.H.Ho,C.P.Chang,F.L.Shyu,R.B.Chen,S.C.Chen,M.F.Lin, *Carbon* 42 (**2004**) 3159

[12] R.Saito,G.Dresselhaus,M.S.Dresselhaus, *J.Appl.Phys.* 73 (**1993**) 494

[13] Y.H.Ho,G.W.Ho,S.J.Wu,M.F.Lin, *J.Vac.Sci.Technol. B* 24 (**2006**) 1098

[14] Ph.Lambin, V.Meunier,A.Rubio, *Phys.Rev.B* 62 (**2000**) 5129

[15] M. Pudlak, R. Pincak and V.A. Osipov, *Phys. Rev. B* 74 (**2006**) 235435

[16] R. Pincak and M. Pudlak, *Progress in Fullerene Research* , Ed. Milton Lang, Nova Science Publisher, ISBN 1-60021-841-5, Chapter 7 (2007) 235-268

[17] R.Saito,G.Dresselhaus and M.S.Dresselhaus, *Physical Properties of Carbon Nanotubes*, Imperial College Press, 2003

[18] J.-C.Charlier, X.Blase,S.Roche, *Review of Modern Physics* 79 (**2007**) 677

[19] R.Saito,M.Fujita,G.Dresselhaus and M.S.Dresselhaus, *Phys.Rev.B* 46 (**1992**) 1804

[20] J.M.Luttinger, *Phys.Rev.* 84 (**1951**) 814

[21] F. Triozon, S. Roche, A. Rubio and D. Mayou, *Phys. Rev. B* 69 (**2004**) 121410(R)

[22] C.H. Lee *et al.*, *J.Phys.:Condens.Matter* 20 (**2008**) 075213

[23] Y.J. Kang and K.J Chang, Y.H. Kim, *Phys. Rev. B* 76 (**2007**) 205441

[24] T.Frankel, *The Geometry of Physics*, Cambridge University Press,Cambridge, 1999

[25] M.Pudlak and R.Pincak, *Eur.Phys.J. B* 67 (**2009**) 565

[26] A.Kleiner, S.Eggert, *Phys.Rev. B* 64 (**2001**) 113402

[27] W.M.Lomer, *Proc. Roy. Soc. A* 227 (**1955**) 330

[28] M.Fujita,K.Wakabayashi,K.Nakada and K.Kusakabe, *J.Phys.Soc.Japan* 65 (**1996**) 1920

[29] M.Pudlak and R.Pincak, *Phys.Rev. A* 79 (**2009**) 033202

[30] D.J.Klein, *Chem.Phys.Lett.* 217 (**1994**) 261

[31] O.Hod and E.Scuseria, *ACS Nano.* 2 (**2008**) 2243

[32] A.G.Souza Filho *et al.*, *NANO LETTERS* 7 (**2007**) 2383

[33] B.Shan,K.Cho, *Phys.Rev.B* 73 (**2006**) 081401(R)

[34] P.N.Dyachkov, D.V.Makaev, *Phys.Rev. B* 74 (**2006**) 155 442